Alterations in Canine Vertebral Bone Turnover, Microdamage Accumulation, and Biomechanical Properties following 1-year Treatment with Clinical Treatment Doses of Risedronate or Alendronate

Matthew R. Allen [1], Ken Iwata [1], Roger Phipps [4], and David B. Burr [1,2,3]

[1] Department of Anatomy and Cell Biology, [2] Department of Orthopaedic Surgery, Indiana University School of Medicine; and [3] Biomedical Engineering Program Indiana University-Purdue University Indianapolis, Indianapolis, IN;

[4] Procter and Gamble Pharmaceuticals, Inc., Mason, OH. 11

Running title: Bone turnover, microdamage, and biomechanics

Corresponding Author:

Matthew R. Allen, Ph.D.

Dept of Anatomy & Cell Biology

635 Barnhill Drive, MS-5035

Indianapolis, IN 46202

Tel: (317) 274-1283

FAX: (317) 278-2040

Email: matallen@iupui.edu

This is the author's manuscript of the article published in final edited form as: Allen M. R., Iwata K., Phipps R., Burr D.B. (2006). Alterations in Canine Vertebral Bone Turnover, Microdamage Accumulation, and Biomechanical Properties following 1-year Treatment with Clinical Treatment Doses of Risedronate or Alendronate *Bone*, 39(4): 872– 9. Available from: http://dx.doi.org/10.1016/j.bone.2006.04.028

Abstract

One year of treatment with bisphosphonates at 5x the dose used for post-menopausal osteoporosis significantly increases failure load and microdamage, and decreases toughness at multiple skeletal sites in intact female beagles. The goal of this study was to determine if similar changes occur with doses equivalent to those used for PMO treatment. Skeletally-mature female beagles were treated daily for one year with vehicle (VEH) or one of three doses of risedronate (RIS; 0.05, 0.10, 0.50 mg/kg/day) or alendronate (ALN; 0.10, 0.20, 1.00 mg/kg/day). Doses of ALN corresponded to treatment dose for PMO, ½ that dose, and 5x that dose on a mg/kg basis; RIS was given at a dose-equivalent to ALN. Vertebral density, geometry, percent ash, static/dynamic histology, microdamage, and biomechanical parameters were quantified. Trabecular bone activation frequency (Ac.f) was dose-dependently lower in RIS-treated groups (-40%, -66%, -84%, $p < 0.05$ vs VEH) while the three ALN groups were all similarly lower compared to VEH (-65%, -71%, -76%; $p < 0.05$). Crack surface density (Cr.S.Dn) was significantly higher than VEH for all doses of RIS and ALN (+2.9 to 5.4-fold vs VEH). Stiffness was significantly increased with both agents while there were no significant changes in any other structural or estimated material properties. Cr.S.Dn and Ac.f exhibited a significant non-linear correlation ($r^2 = 0.21$; $p<0.001$) while there was no relationship between Cr.S.Dn and any mechanical properties. These results document that 1-year of bisphosphonate treatment at clinical doses allows significant accumulation of microdamage in the vertebra but this is offset by increases in bone volume and mineralization such that there is no significant impairment of mechanical properties. 45

Key words: bisphosphonate, remodeling, histomorphometry, osteoporosis

INTRODUCTION

Anti-remodeling drugs reduce fracture risk by altering both structural and material bone properties [1]. Suppressed bone remodeling enhances bone structure through increases in bone volume and maintenance of trabecular architecture [2, 3]. At the material level, remodeling suppression increases average tissue mineralization and tissue density homogeneity [4]. Biomechanically, these structural and material changes enhance whole bone strength and stiffness, yet increased mineralization is also negatively correlated to toughness [5-7]. A greater understanding of the net balance among structural and material alterations that occur with anti-remodeling treatment is necessary.

We and others have documented that bisphosphonate administration at 5x the clinical dose for treatment of post-menopausal osteoporosis, increases trabecular bone volume, mineralization, ultimate load and stiffness in dog vertebra [8, 9]. However, remodeling suppression to levels produced by these doses also significantly increases microdamage accumulation and decreases bone toughness [8, 9]. These previous studies were designed to examine the role of remodeling suppression on microdamage and biomechanical properties, rather than the effects of individual bisphosphonate treatments, which have demonstrated anti-fracture efficacy [10]. The results have raised some concerns about long-term anti-remodeling therapies [11, 12], but the applicability of these data to clinical situations remains unclear because the bisphosphonate doses were 5- to 6-times the clinical dose used for treatment of post-menopausal osteoporosis. Although the degree of remodeling suppression in these dog studies was similar to that of post-menopausal women [13], it may represent over-suppression in a non-osteoporotic dog model that has slower bone turnover compared to

post-menopausal women. It is possible that the microdamage and toughness changes in the dog model are specific to the high doses used in these previous studies.

The objective of this study was to quantify the changes in bone remodeling, microdamage accumulation, and biomechanical properties following 1-year treatment with bisphosphonate doses equivalent to those used for prevention/treatment of post-menopausal osteoporosis. Our hypothesis was these clinical treatment doses would allow significant increases in microdamage accumulation and reductions in toughness due to suppression of bone remodeling. To test this hypothesis, skeletally mature female beagle dogs were treated daily for 1 year with either risedronate or alendronate at the clinical treatment dose (0.10 and 0.20 mg/kg/day p.o, respectively), as well as lower and higher doses so that dose-response effects for damage accumulation and toughness could also be determined. Density, geometry, mineralization, remodeling, microdamage, and biomechanical properties of vertebral bone were quantified. 82

MATERIALS AND METHODS

Animals

Eighty-four skeletally mature female beagles (1.3 ± 0.02 years old) were purchased from Marshall Farms USA (North Rose, NY). Upon arrival, lateral X-rays of all dogs were obtained to confirm skeletal maturity (closed proximal tibia and lumbar vertebra growth plates). Animals were housed two per cage in environmentally controlled rooms at Indiana University School of Medicine's AALAC accredited facility and provided standard dog chow and water. All procedures were approved prior to the study by the Indiana University School of Medicine Animal Care and Use Committee.

Experimental Design

Following two weeks of acclimatization, animals were assigned to treatment groups (n=12/group) by matching body weights. All dogs were treated daily for 1-year with oral doses of vehicle (saline), risedronate sodium (Procter and Gamble Pharmaceuticals, Inc) or alendronate sodium (Merck and Co., Inc). Alendronate doses (0.10, 0.20, and 1.00 mg/kg/day) were chosen to correspond with clinical doses used for post-menopausal osteoporosis. The lower two doses are equivalent (on a mg/kg basis) to the preventative (5 mg) and therapeutic (10 mg) doses of alendronate. Based on the ratios of in vivo potency (1:2) and clinical dose levels (2:1), dose-equivalents of risedronate were administered at doses of 0.05, 0.10, and 0.50 mg/kg/day. Both risedronate and alendronate were dissolved in saline and administered to the dogs orally with a syringe. Vehicle-treated animals received 1 ml/kg/day of saline. Dosing was performed each morning after an overnight fast and at least 2 hours prior to feeding.

Prior to necropsy, animals were injected with calcein (0.20 mL/kg, IV) using a 2-12-2-5 labeling schedule (9 animals per group) or a 2-5-2-5 (3 animals per group). The shorter interlabel duration was due to a scheduling error. Animals were euthanized by intravenous administration of sodium pentobarbital (0.22mg/kg Beuthanasia-D Special). After death, thoracic and lumbar vertebrae were dissected and saved for analyses. The ninth thoracic and fourth lumbar vertebrae were separately wrapped in saline-soaked gauze and frozen (-20ºC). Second and third lumbar vertebrae were fixed in 10% neutral buffered formalin.

Densitometry

Areal bone mineral density (aBMD, g/cm^2) of the fourth lumbar vertebra (L4) was quantified using a PIXImus II densitometer (Lunar Corp.). Prior to scanning, the vertebrae were thawed

to room temperature. The posterior elements and cranial/caudal endplates were removed using a low speed diamond saw (Labcut 1010, Extec) under constant irrigation. Endplate removal was done such that surfaces were parallel for mechanical testing. Scanning (0.18x 0.18 mm/pixel) was performed with the vertebral body laying on its medial surface. For each specimen, aBMD of the entire vertebral body, excluding the posterior elements, was determined.

Volumetric bone density and geometry of the L4 vertebra was quantified using a Norland Stratec XCT Research SA+ pQCT (Stratec Electronics). A scout view of each bone was obtained to determine slice locations. One slice (0.07 X 0.07 x 0.50 mm voxel size) was taken at three locations (25, 50 and 75% of total vertebra height). Total and trabecular volumetric bone mineral density (vBMD, mg/cm^3) and cross-sectional area (CSA, mm^2) were obtained for each slice using contour mode 1, peel mode 2, and a threshold of 710 mg/cm^3. Values from the three slices were averaged together to obtain a single representative value for each specimen.

Percent Ash

Percent ash was quantified from two regions of the ninth thoracic vertebrae. Vertebrae were thawed to room temperature and cut in half using a band saw (Marmed Inc.) under constant irrigation. The caudal half was saved whole while a trabecular bone core (4 mm^3) was cut from the mid-cranial metaphysis. Specimens were dried using acetone/anhydrous ether and weighed daily until mass was stabilized for two consecutive days (dry weight). Bones were ashed at 800ºC for 12 hours using a 1400 Thermolyne oven (Barnstead). Ashed specimens were allowed to cool and then weighed (ash weight). Percent ash was calculated as ash weight/dry weight * 100.

Histology (Static, dynamic, and microdamage)

Static and dynamic histomorphometric measures of trabecular bone were obtained on second lumbar vertebrae. After 3 days of fixation, bones were transferred to 70% ethanol until processing. Using an automatic tissue processor (Shandon/Lipshaw), specimens were cycled through a graded series of ethanols, cleared using xylene, and infiltrated with methyl methacrylate (MMA; Aldrich). Specimens were transferred to a solution of MMA + 3% dibutyl phthalate (DBP; Sigma-Aldrich) for 3-7 days under vacuum and then embedded using MMA + DBP + 0.25% catalyst (Perkadox 16^3; Akzo Nobel Chemicals). Mid-sagittal (4 µm) sections were cut using a Reichert-Jung 2050 microtome (Magee Scientific, Inc) and stained with McNeal's tetrachrome for static histomorphometry. Mid-sagittal (8 µm) sections were cut and left unstained for dynamic histomorphometry and wall thickness measures.

Third lumbar vertebrae were processed for microdamage assessment by bulk staining in basic fuchsin [14]. Using 1% basic fuchsin dissolved in increasing concentrations of ethanol, specimens were stained according to the following schedule: 8 hours 80% (with one change to fresh 80% after 4 hours), overnight in 95% (with one change to fresh 95%), 8 hours in 100% (with one change to fresh 100% after 4 hours). Bones were placed under vacuum (20 in Hg) for all stages during the day and left on the bench top overnight. Following staining, bones were washed 2x in 100% ethanol (five minutes each), placed in 100% MMA under vacuum for 4 hours, and then transferred to MMA + DBP for 3 days. Samples were embedded in MMA + DBP + 0.25% catalyst. Mid-sagittal (80-100 µm) sections were cut using a diamond wire saw (Histosaw; Delaware Diamond Knives).

Histological measurements were made using a semiautomatic analysis system (Bioquant OSTEO 7.20.10, Bioquant Image Analysis Co.) attached to a microscope equipped with an ultraviolet light source (Nikon Optiphot 2 microscope, Nikon). Measurements were carried out on one stained (static), one unstained (dynamic), and two bulk stained (microdamage) sections per animal. Analysis of a single stained and unstained section has been previously shown to be sufficient to detect significant differences in this animal model [8] while two sections were measured for microdamage variables to reduce the probability of crackless specimens [15]. A 5 x 5 mm region of interest, located 1 mm below the cranial plateau, was used for sampling. Static and dynamic variables were measured and calculated in accordance with ASBMR recommended standards [16]. Microdamage was assessed using UV fluorescence as previously described [17]. Cracks were identified by their typical linear shape, relative size (greater than canaliculi, smaller than vascular channels), and positive fluorescence (due to diffusion of stain into the crack wall) (Figure 1). Microcracks were identified at 10x magnification and measured at 20x magnification. Measurements included crack length (Cr.Le, µm) and crack number (Cr.N), with calculations of crack density (Cr.Dn, #/mm^2; Cr.N / bone area) and crack surface density (Cr.S.Dn, µm/mm^2; Cr.N * Cr.Le / bone area).

Biomechanical Testing

The biomechanical properties of fourth lumbar vertebrae were quantified using a servohydraulic testing system (MTS 810, MTS Corporation). Following densitometry, vertebral height was measured using digital calipers (Starrett #721; L.S. Starrett Co). Compression to failure was carried out on saline soaked specimens using displacement control mode (20 mm/min). Load vs displacement curves were recorded using a HP-7090

plotting system. Plots were analyzed for determination of ultimate force (maximum force obtained during test) and stiffness (slope of the linear portion of load/displacement curve). Work to ultimate force (area under the load/displacement curve before ultimate force) was measured by digitizing plots and analyzing the area using standard imaging software (Scion Image; Scion Corp.). Ultimate stress (σ_{ult}), modulus (E), and toughness (U) were estimated using the following equations:

$$\sigma_{ult} = (\text{ultimate force} / \text{CSA}) / \text{BV/TV}$$

$$E = (\text{stiffness} * (\text{height} / \text{CSA})) / \text{BV/TV}$$

$$U = (\text{work to ultimate force} / (\text{height} * \text{CSA})) / \text{BV/TV}$$

where cross sectional area is from pQCT measures of the same vertebrae (L4), height measured using digital calipers, and BV/TV from L2 histomorphometry. These equations have been previously used to estimate the material properties of canine vertebra [8, 9].

Statistics

All statistical tests were performed using SAS software (SAS Institute, Inc.). Differences among all seven treatment groups were evaluated using a one-way analysis of variance (ANOVA), allowing evaluation between RIS and ALN at dose-equivalents. Additionally, separate ANOVAs were run for VEH+RIS and VEH+ALN to independently compare each drug (and dose) to vehicle-treated animals. When a significant overall F value ($p < 0.05$) was present, differences between individual group means were tested using Fisher's protected least-significant difference (PLSD) post-hoc test. Simple linear or polynomial regression analyses were performed to test the relationship among activation frequency, percent ash, crack surface density, and toughness. For all tests, $p \leq 0.05$ was considered statistically significant. All data are presented as mean ± standard error.

RESULTS

There was no difference (both $p > 0.90$) among group body masses at baseline (overall average 8.30 ± 0.14 kg) or at the conclusion of the treatment (overall average 8.97 ± 0.16 kg). All animals completed the one year of treatment without observable complication from the drugs. Two dosing errors occurred during the study. One dog in the high dose risedronate group (0.50 mg/kg/day) received a different drug (raloxifene, 0.5 mg/kg/day) for 2 days in the month prior to sacrifice. One dog in the low dose alendronate group (0.10 mg/kg/day) received the middle dose risedronate (0.10 mg/kg/day) for the entire 5th month of treatment. These animals remained in all analyses as the values were within the variance of their respective groups.

Density, geometry, mineralization

Areal bone mineral density (aBMD, g/cm^2) was not significantly increased with treatment ($p = 0.07$; Table 1) while volumetric total bone mineral density (vBMD, mg/cm^3) and volumetric trabecular BMD were both significantly increased compared to VEH (Table 1). Total vBMD was significantly higher ($p = 0.03$) than VEH for the middle and high doses of ALN while trabecular vBMD was significantly higher ($p = 0.02$) for the middle and high doses of RIS. There was no significant difference between any dose-equivalents of RIS and ALN, or within drug at the various doses, for any of the density variables. Total cross-sectional area of the vertebral body was not significantly changed with either RIS or ALN. Trabecular bone percent ash was significantly higher (+ 3 to +5 %) than VEH for the middle and high doses of RIS and all three doses of ALN (Table 1). Cortical plus trabecular bone percent ash was not significantly different than vehicle for RIS or ALN (+1 to +3% vs

vehicle). There was no difference among doses within drug, or between drugs at dose-equivalents, for percent ash.

Static and dynamic histomorphometry

Trabecular bone volume (BV/TV) was significantly higher with bisphosphonate treatment (Table 2). The low and high doses of RIS and all three doses of ALN were significantly higher than VEH (+5 to + 21%). Activation frequency (Ac.f) was significantly lower than vehicle-treated animals in all bisphosphonate-treated groups (Figure 2). The suppression of Ac.f was significantly less (-40%) in the low dose RIS group compared to both middle and high doses (-66 and -84%, respectively). Ac.f was also significantly higher in the low dose RIS group compared to its ALN dose-equivalent. All ALN groups had significantly lower Ac.f compared to vehicle (-65% to -76%) with no difference among the three doses. Activation frequency suppression resulted from reduced bone formation rate (BRF/BS) in all bisphosphonate groups; there was no significant difference in mean wall thickness among groups (Table 2). Reduced BFR/BS (-38 to -81%) resulted from a significant reduction in mineralizing surface (MS/BS); mineral apposition rate was not different among groups although it tended to be lower with both RIS ($p = 0.07$) and ALN ($p = 0.06$) compared to VEH. Risedronate dose-dependently suppressed MS/BS (-26, -51, and -75% for 0.05, 0.10, 0.50 doses, respectively); all three ALN doses were similarly lower than vehicle-treated animals (-49 to -69%). MS/BS of the low dose RIS group was significantly higher than its dose-equivalent of ALN. There was a significant negative linear relationship ($r^2 = 0.13$; $p = 0.008$) between Ac.f and % ash of trabecular bone (%ash = -1.08(Ac.f) + 63.61).

Microdamage accumulation

Risedronate and alendronate each increased the number of microcracks in vertebral trabecular bone, with no effect on mean crack length (Table 3). Crack density (Table 3) was significantly higher in all RIS-treated groups compared to VEH; the highest dose was significantly higher than both the low and middle dose of RIS. The middle and high doses of ALN had significantly higher Cr.Dn compared to VEH; the highest dose was significantly greater than the lowest dose. Crack surface density (Figure 2) differences were similar to those of Cr.Dn. All three RIS groups had significantly higher Cr.S.Dn compared to VEH (+2.9 to +5.4-fold vs VEH) with the highest dose significantly higher than the lower two doses. ALN groups were all significantly higher than VEH (+3.1 to +4.7-fold vs VEH) with no significant difference among the doses. There was a significant negative non-linear relationship ($Cr.S.Dn = 1.469 – 0.47(Ac.f) + 0.0005(Ac.f)^2$; $r^2 = 0.21$; $p<0.001$) between Cr.S.Dn and Ac.f (Figure 3); this relationship was similar for each drug separately. There was no difference in microdamage parameters between drugs at dose-equivalents.

Biomechanical properties

Neither ultimate load nor ultimate stress was significantly different among groups (Table 4). Stiffness was significantly higher than vehicle with both RIS (middle and high doses) and ALN (all three doses), while modulus was not significantly different among groups. There was no significant difference among groups in work to ultimate load or toughness (Table 4). There was no correlation between toughness and crack surface density ($r^2 = 0.006$; $p = 0.46$).

DISCUSSION

One-year of bisphosphonate treatment at doses equivalent to 5x the clinical dose for post-menopausal osteoporosis suppresses remodeling and increases trabecular bone volume, mineralization and stiffness in dogs [8, 9]. However, remodeling suppression to levels produced by these high doses also significantly increases microdamage accumulation and decreases toughness [8, 9]. These findings led to numerous questions regarding the relationship between remodeling suppression, microdamage, and biomechanical properties. The current study allows us to address specifically: 1) whether the extent of damage accumulation is related to the degree of remodeling suppression; 2) whether a level of remodeling suppression exists that allows targeted remodeling to limit microdamage accumulation; and 3) whether doses of risedronate or alendronate that are equivalent to those used for treatment of post-menopausal osteoporosis increase microdamage accumulation and decrease toughness in canine vertebra.

Site-specific variations in microdamage have led to the proposal that the amount of damage accumulation is related to the level of remodeling suppression [18]. On an individual sample basis, the relationship between remodeling suppression and damage accumulation was significantly related in a non-linear fashion (r^2 =0.21), similar to previous reports [8, 9]. However on a population basis (within individual treatment groups) a wide range of remodeling suppression (-40 to -84%) was associated with equivalent microdamage accumulation. For example, two treatment groups with significantly different reductions in activation frequency (RIS 0.05 (-40%) and RIS 0.10 (-66%)) both had a 2.9-fold increase in crack surface density. Conversely, two groups with roughly equivalent decreases in remodeling (ALN 0.2 (-71%) and ALN 1.0 (-76%)) had quite different crack surface

densities (+ 3.7 and + 4.7-fold higher than vehicle). These data suggest that, although as a general rule remodeling suppression increases microdamage, in treatment populations the extent of remodeling suppression is a poor marker of the amount of microdamage accumulation. This may be due to other factors that occur secondary to remodeling suppression (e.g. a change in matrix mineralization) that may play a larger role in determining microdamage accumulation than previously hypothesized [19, 20]. Alternatively, it could represent individual biological response to treatment, similar to findings in clinical trials [21, 22]. These studies have documented populations of "responders" and "non-responders" to bisphosphonate treatment as assessed using BMD and bone turnover biomarkers. Similar variability is plausible in animals (and humans) with respect to turnover suppression and microdamage accumulation.

It has been suggested that remodeling suppression of less than 50% may limit microdamage accumulation [23, 24] by allowing a sufficient amount of targeted remodeling [25, 26]. In the current study only the lowest dose of risedronate (equivalent to half the dose for PMO treatment) reduced activation frequency less than this proposed threshold (-40% compared to vehicle). Crack surface density in this group was significantly higher (3-fold) than vehicle-treated animals, and not significantly different than the middle RIS dose or the dose-equivalent of ALN. Therefore, even mild suppression of trabecular bone remodeling in this canine model allows significant damage accumulation suggesting the threshold is below a 40% reduction. The level of remodeling suppression that allows microdamage accumulation may differ in post-menopausal women who have increased bone turnover prior to bisphosphonate treatment and likely differs depending on whether measured by histology or biomarkers.

It is well-accepted that bisphosphonates decrease fractures in at-risk populations [10, 27-30]. The current study supports these clinical observations by documenting non-significantly higher ultimate load and significantly higher vertebral stiffness in animals treated with RIS or ALN at doses equivalent to those used for treatment of post-menopausal osteoporosis. These enhanced structural properties, manifested through changes in bone density (bone volume and mineralization), are likely the mechanism responsible for large reduction in fracture risk. There was no significant difference among groups in energy to ultimate load or in any of the estimated material properties. It is important to note that these data represent estimated material properties, having different absolute values compared to those from isolated trabecular bone cores. However, values are comparable with previous studies in dog vertebra from our lab and others [8, 9, 18, 31]. Taken together, these data suggest an overall positive effect of bisphosphonate treatment at clinical dosing equivalents on the structural but not the material properties of vertebral bone.

The absence of significant reductions in toughness, given the significant increase in microdamage accumulation, contradicts previous results that implicated microdamage accumulation as a principal determinant of toughness reduction with bisphosphonate treatment [8, 9, 18, 31]. These previous studies all utilized bisphosphonate doses that exceeded the clinical treatment dose by 2.5 to 6 times, suggesting that toughness reductions may be confined to high bisphosphonate dosing levels. Indeed, when the high dose groups of the current study are individually compared to VEH the differences in toughness approach, although still do not achieve, statistical significance compared to VEH (ALN, $p = 0.06$; RIS, $p = 0.20$). As a percent of VEH values, changes in the high dose groups (-13 and -17% for RIS 0.5 and ALN 1.0, respectively) were slightly less than our previous studies (-20%

compared to VEH) [8]. Based on these results it appears the toughness reductions with bisphosphonate treatment may be specific to some change brought about by high-dose regimens. However, it is hard to ignore the consistency of the non-significantly lower toughness values in all treatment groups compared to vehicle (-6 to -17%). The absence of relationship between crack surface density and toughness suggests that factors other than damage accumulation may be principally responsible for the reductions in toughness previously reported with bisphosphonate treatment [8, 9, 18].

Alendronate and risedronate are both nitrogen-containing bisphosphonates approved for treatment of post-menopausal osteoporosis (PMO). A head-to-head clinical trial has shown different degrees of BMD and biomarker changes with these two agents [21]. These two bisphosphonates have also been documented to exhibit different bone pharmacokinetic and binding properties [32, 33]. In the current study, we evaluated both drugs at various dose-equivalents based on the lower in vivo potency (1:2) and higher clinical dosing (2:1) of ALN vs RIS. Histological markers of bone turnover (MS/BS, BFR/BS and Ac.F) were suppressed significantly less in RIS-treated animals compared to the dose-equivalent of ALN at the lowest dose. In addition RIS demonstrated dose-dependency in Ac.f compared to ALN which decreased remodeling similarly at all three doses. At the lowest dose, equivalent on a mg/kg basis to the dose prescribed for prevention of post-menopausal osteoporosis, ALN suppressed Ac.f by 65%, not different from the 76% suppression at a dose 10x higher. Suppression of Ac.f with RIS more than doubled (-40 % to -84%; $p < 0.05$) between the lowest and the highest doses. This suggests risedronate has a greater ability to finely regulate bone remodeling, a quality that may be beneficial in situations in which smaller reductions in turnover would be advantageous. Trabecular bone volume (BV/TV) was also significantly

different for the middle dose of the two drugs, with RIS being significantly lower than ALN. The reason for this is unclear but we believe it is not likely a true biological effect given that other skeletal sites in these dogs, such as the femoral neck, show increased BV/TV comparable to the dose-equivalent of ALN (data not shown).

The results of this study should be considered in light of various limitations. Use of intact, non-ovariectomized beagle dogs may limit the translation of these results to high turnover, low bone mass conditions such as post-menopausal osteoporosis. The interaction between estrogen-deficiency and bisphosphonate treatment is difficult to assess in dogs due to their low baseline estrogen levels and their failure to lose trabecular bone via increased remodeling with ovariectomy [34]. Our quantification of bone turnover and microdamage were confined to trabecular bone of the vertebral body while biomechanical properties were assessed for the entire vertebral body. It is possible that changes in the cortical shell, such as in bone turnover, microdamage, and/or other properties contributed to the biomechanical changes, although there was no significant change in cortical shell BMD assessed by pQCT (data not shown).

The aim of this study was to determine the effects of bisphosphonate treatment at doses equivalent to those used for post-menopausal osteoporosis on various properties of canine vertebrae. Based on our results, we conclude that: 1) microdamage accumulation with bisphosphonate treatment is related to remodeling suppression in a non-linear fashion on an individual, but not population, basis; 2) suppression of remodeling by 40% with bisphosphonate treatment is still sufficient to allow significant accumulation of microdamage in the vertebra; and 3) although clinical treatment doses of alendronate and risedronate used for post-menopausal osteoporosis significantly increase microdamage accumulation after 1

year, enhanced bone volume and mineralization resulted in no significant impairment of mechanical properties in this canine model.

Acknowledgements

The authors thank Dr. Keith Condon, Diana Jacob, Mary Hooser, and Lauren Waugh for histological preparation and Dr. Charles Turner for his assistance with mechanical testing. This work was supported by NIH Grants 5R01AR047838 and 5T32AR007581 and a research grant from The Alliance for Better Bone Health (Procter & Gamble Pharmaceuticals and sanofi-aventis). Merck and Co. kindly provided the alendronate. This investigation utilized an animal facility constructed with support from Research Facilities Improvement Program Grant Number C06RR10601 from the NIH National Center for Research Resources.

Address reprint requests to:

David B. Burr, PhD
Dept. of Anatomy and Cell Biology, MS 5035
Indiana University School of Medicine
635 Barnhill Dr.
Indianapolis, IN 46202

Tel: 317-274-7496
FAX: 317-278-2040
Email: dburr@iupui.edu

FIGURE 1: Microcrack stained en block with basic fuchsin viewed under UV fluorescence. Vertebral microcracks were identified at 10x magnification (A) and measured at 20x magnification (B). Scale bars = 100 µm.

FIGURE 2: Activation frequency and microdamage accumulation of vertebral trabecular bone. (A) Activation frequency was significantly lower than vehicle in all bisphosphonate-treated animals ($p < 0.001$). Risedronate (RIS) produced a dose-dependent suppression while alendronate (ALN) similarly suppressed activation frequency among the three doses. The lowest dose of RIS was significantly different from its ALN dose-equivalent. (B) Crack surface density was significantly higher than vehicle in all bisphosphonate-treated groups ($p = 0.002$). Both clinical doses of RIS were significantly lower than the highest dose; all three ALN doses were similarly higher than vehicle. There were not differences between equivalent doses of RIS and ALN. Data expressed as mean ± SE. Values within each bar represent percent (A) or fold (B) difference vs vehicle. $p < 0.05$ versus vehicle (a); vs low dose within drug (b); vs middle dose within drug (c); vs dose equivalent (d).

FIGURE 3: Non-linear regression analysis between activation frequency (Ac.f) and crack surface density (Cr.S.Dn) in the lumbar vertebra. Decreased activation frequency is associated in a quadratic function with an increase in microdamage accumulation ($p < 0.001$).

References

Delmas, P. D. How does antiresorptive therapy decrease the risk of fracture in women with osteoporosis? Bone 27*:*1-3; 2000.

Dufresne, T., Chmielewski, P., Manhart, M., Johnson, T., and Borah, B. Risedronate Preserves Bone Architecture in Early Postmenopausal Women In 1 Year as Measured by Three-Dimensional Microcomputed Tomography. Calcif Tissue Int 73*:*423-32; 2003.

Rodan, G. A., and Fleisch, H. A. Bisphosphonates: mechanisms of action. J Clin Invest 97*:*2692-6; 1996.

Boivin, G. Y., Chavassieux, P. M., Santora, A. C., Yates, J., and Meunier, P. J. Alendronate increases bone strength by increasing the mean degree of mineralization of bone tissue in osteoporotic women. Bone 27*:*687-94; 2000.

Currey, J. D., Brear, K., and Zioupos, P. The effects of ageing and changes in mineral content in degrading the toughness of human femora. J Biomech 29*:*257-60; 1996.

Currey, J. D. Tensile yield in compact bone is determined by strain, post-yield behaviour by mineral content. J Biomech 37*:*549-56; 2004.

Les, C. M., Stover, S. M., Keyak, J. H., Taylor, K. T., and Kaneps, A. J. Stiff and strong compressive properties are associated with brittle post-yield behavior in equine compact bone material. J Orthop Res 20*:*607-14; 2002.

Mashiba, T., Turner, C. H., Hirano, T., Forwood, M. R., Johnston, C. C., and Burr, D. Effects of suppressed bone turnover by bisphosphonates on microdamage accumulation and biomechanical properties in clinically relevant skeletal sites in beagles. Bone 28*:*524-31; 2001.

Komatsubara, S., Mori, S., Mashiba, T., Ito, M., Li, J., Kaji, Y., Akiyama, T., Miyamoto, K., Cao, Y., Kawanishi, J., and Norimatsu, H. Long-term treatment of incadronate disodium accumulates microdamage but improves the trabecular bone microarchitecture in dog vertebra. J Bone Miner Res 18*:*512-20; 2003.

Bone, H. G., Hosking, D., Devogelaer, J.-P., Tucci, J. R., Emkey, R. D., Tonino, R. P., Rodriguez-Portales, J. A., Downs, R. W., Gupta, J., Santora, A. C., Liberman, U. A., and the Alendronate Phase III Osteoporosis Treatment Study Group Ten Years' Experience with Alendronate for Osteoporosis in Postmenopausal Women. N Engl J Med 350*:*1189-1199; 2004.

Delmas, P. D., and Seeman, E. Changes in bone mineral density explain little of the reduction in vertebral or nonvertebral fracture risk with anti-resorptive therapy. Bone 34*:*599-604; 2004.

Seeman, E. The structural and biomechanical basis of the gain and loss of bone strength in women and men. Endocrinol Metab Clin North Am 32*:*25-38; 2003.

Chavassieux, P. M., Arlot, M. E., Reda, C., Wei, L., Yates, A. J., and Meunier, P. J. Histomorphometric assessment of the long-term effects of alendronate on bone quality and remodeling in patients with osteoporosis. J Clin Invest 100*:*1475-80; 1997.

Burr, D. B., and Stafford, T. Validity of the bulk-staining technique to separate artifactual from in vivo bone microdamage. Clin Orthop Relat Res*:*305-8; 1990.

Martin, B., Fyhrie, D. P., and Yeh, O. C. Sampling bones for microcracks. Trans Orthop Res Soc 30*:*Abstract 1540; 2005.

Parfitt, A., Drezner, M., Glorieux, F., Kanis, J., Malluche, H., Meunier, P., Ott, S., and Recker, R. Bone histomorphometry: Standardization of nomenclature, symbols, and units. Journal of Bone and Mineral Research 2*:*595-610; 1987.

Huja, S. S., Hasan, M. S., Pidaparti, R., Turner, C. H., Garetto, L. P., and Burr, D. B. Development of a fluorescent light technique for evaluating microdamage in bone subjected to fatigue loading. J Biomech 32*:*1243-9; 1999.

Mashiba, T., Hirano, T., Turner, C. H., Forwood, M. R., Johnston, C. C., and Burr, D. Suppressed bone turnover by bisphosphonates increases microdamage accumulation and reduces some biomechanical properties in dog rib. J Bone Miner Res 15*:*613-20; 2000.

Norman, T. L., and Wang, Z. Microdamage of human cortical bone: incidence and morphology in long bones. Bone 20*:*375-9; 1997.

O'Brien, F. J., Taylor, D., and Clive Lee, T. The effect of bone microstructure on the initiation and growth of microcracks. J Orthop Res 23*:*475-80; 2005.

Rosen, C. J., Hochberg, M. C., Bonnick, S. L., McClung, M., Miller, P., Broy, S., Kagan, R., Chen, E., Petruschke, R. A., Thompson, D. E., and de Papp, A. E. Treatment with once-weekly alendronate 70 mg compared with once-weekly risedronate 35 mg in women with postmenopausal osteoporosis: a randomized double-blind study. J Bone Miner Res 20*:*141-51; 2005.

Sebba, A. I., Bonnick, S. L., Kagan, R., Thompson, D. E., Skalky, C. S., Chen, E., and de Papp, A. E. Response to therapy with once-weekly alendronate 70 mg compared to once-weekly risedronate 35 mg in the treatment of postmenopausal osteoporosis. Curr Med Res Opin 20*:*2031-41; 2004.

Burr, D. Microdamage and bone strength. Osteoporos Int 14 Suppl 5*:*67-72; 2003.

Li, J., Sato, M., Jerome, C., Turner, C. H., Fan, Z., and Burr, D. B. Microdamage accumulation in the monkey vertebra does not occur when bone turnover is suppressed by 50% or less with estrogen or raloxifene. J Bone Miner Metab 23 Suppl*:*48-54; 2005.

Burr, D. B., Martin, R. B., Schaffler, M. B., and Radin, E. L. Bone remodeling in response to in vivo fatigue microdamage. J Biomech 18*:*189-200; 1985.

Martin, R. B. Is all cortical bone remodeling initiated by microdamage? Bone 30*:*8- 13; 2002.

Black, D. M., Cummings, S. R., Karpf, D. B., Cauley, J. A., Thompson, D. E., Nevitt, M. C., Bauer, D. C., Genant, H. K., Haskell, W. L., Marcus, R., Ott, S. M., Torner, J. C., Quandt, S. A., Reiss, T. F., and Ensrud, K. E. Randomized trial of effect of alendronate on risk of fracture in women with existing vertebral fractures. Fracture Intervention Trial Research Group. Lancet 348*:*1535-41; 1996.

Delmas, P. D., Li, Z., and Cooper, C. Relationship between changes in bone mineral density and fracture risk reduction with antiresorptive drugs: some issues with meta- analyses. J Bone Miner Res 19*:*330-7; 2004.

Cummings, S. R., Black, D. M., Thompson, D. E., Applegate, W. B., Barrett-Connor, E., Musliner, T. A., Palermo, L., Prineas, R., Rubin, S. M., Scott, J. C., Vogt, T., Wallace, R., Yates, A. J., and LaCroix, A. Z. Effect of alendronate on risk of fracture in women with low bone density but without vertebral fractures: results from the Fracture Intervention Trial. JAMA 280*:*2077-82; 1998.

Cummings, S. R., Karpf, D. B., Harris, F., Genant, H. K., Ensrud, K., LaCroix, A. Z., and Black, D. M. Improvement in spine bone density and reduction in risk of vertebral fractures during treatment with antiresorptive drugs. Am J Med 112*:*281-9; 2002.

Komatsubara, S., Mori, S., Mashiba, T., Li, J., Nonaka, K., Kaji, Y., Akiyama, T., Miyamoto, K., Cao, Y., Kawanishi, J., and Norimatsu, H. Suppressed bone turnover by long-term bisphosphonate treatment accumulates microdamage but maintains intrinsic material properties in cortical bone of dog rib. J Bone Miner Res 19*:*999- 1005; 2004.

Christiansen, C., Phipps, R., Burgio, D., Sun, L., Russell, D., Keck, B., Kuzmak, B., and Lindsay, R. Comparison of risedronate and alendronate pharmacokinetics at clinical doses. Osteoporos Int 14*:*S38; 2003.

Nancollas, G. H., Tang, R., Phipps, R. J., Henneman, Z., Gulde, S., Wu, W., Mangood, A., Russell, R. G., and Ebetino, F. H. Novel insights into actions of bisphosphonates on bone: Differences in interactions with hydroxyapatite. Bone; 2005.

Shen, V., Dempster, D. W., Birchman, R., Mellish, R. W., Church, E., Kohn, D., and Lindsay, R. Lack of changes in histomorphometric, bone mass, and biochemical parameters in ovariohysterectomized dogs. Bone 13*:*311-6; 1992.

Table 1

Click here to do'''''''loaj high resolution image

Tabl•1: Density, geometry, and percntsh or fourth lumbar ertebrn

	\I!hk!!,	R.l;tedrolt(mJ.-lWfl			.ui:... ıı0.-.t:e-'*'1)					
T C C l.l•&MD	ffitlS					Q.:O			A U i	
	t.JJ .tOtll	tl "a:OtlJ	0))a:tOI	tiJ6:t.0(11	f ,_..tO OI	G:N .tOtll	0 »:t.f tl1			
		606:t.IJ	601.t'		001.tII	Qf .t''	6''11)•			0''
Tr•bt	}ıı t1	J.:SatS	)Qt••	3171•'			>S-3l7			
CSA	11'1ts	lff.t<ıı	113.t6	Illts	)61'.ts 111.tf	U4t4	111l)			
	601-.il6	QS.:.tS	00.it••	C•.t.06•	'1& .t.O.S•	fl.0.:06•	637.tt.5•			0''
	sa1.it•	Sl7t.lS	StI .ti?	-"3t.06	5aS.t.OS	'1.:.0..6	601.tlS			

Arttl bone 111.iMnl dtmily (aBMD) oftbt,trttbntlbod)' uscsstd usina pDXA dauilocortry. Total and cmccllous \'Cdumm:k bont udne1t dtiwily (VB1D) . 1ot•I tt0:tteelionel art1daenn ned by pQCT M1.S.50,er1d 75911

O(\•c:rttbnll1t'8JJl:''8JJhOflrnb«'u1trbOlleC()ll't · klftslioc- O(Vtrtcbclt (COrtit-al +hblll•)dt'letutiue(f b)' ashklg._ Dato artmtan tse. Stpmitt I 'A•Y ANOVA nm using V£H+1US or A1.N 10 dttttminci di1ftttlltt:S lfDOllg <klllet .d vddck (•V1vdliclt), ANOVA ttl!:i111&lJgr med 10 dccmnin dlflcrtoca 11 dote-eqm•1knls(no do6e--tqUiv 1kn1 ciffn-ctK for tbeet 'ari1bJell).

Table 2

Click here to do"""""loaj high resolution image

Table 2: Trnb•cufar histomorph om•lry of S<>cond lumbar Yer1cbra

	\' • •		... - qtcbl,r)		All':.....11 ems."				VD<•	V?H• ALI'
			OJO		OJO					
evnV.v.	1lt 1U	H'.tll•	2l01JJ•	261j1•	lS?t J S•	M'.tI O•	U.9 11)•	;ʊ ..		
WTh,..	641StJI	'71:tl''	17, a. JI	,.....t,..	1'1't''l	"140&11	1''t2f		•, •	
	1'4.tOIO	I1l t 0 1l	l t• tDIO	1lOt O l''	lll tD11	l lS tO OJ	11'1&01l			
	lJ 111•	IS1.:.12..	IDS.ti••	Sl.tl l•	tll l t !1•	10 I .:.I $•	•lt !O•		ctOlll	cQllDI
,,,,,_W	tʊ	,.t 11""	•S.t*	D.t6..	'Itcl•	!.16.	Jl.t6 -			<0 Olll

CUl<'dlOl>tl bocll'\0IWllC'(BVfT'V)liSC8SC'dOCIL2\crttbraeU5ingMtNttllt'l11LC1bOO!oC'At.in. Oyoatok IDCtill"tl from Ullll!'ltai:tC"d\tttt'bl'Ml m«llou.s boM. Wb, "'alltbkknc-n; MAR.. o*1cn.J apposition 1111c:. ISIBS.miocrlllizing 1altf•ce: OFRJl)S,bone (onnotion t'llc-. 1.>11••eniean ± SE. Stp1ra1el'"wrf.'-*.OV/\ntn ut:ing Vf,JJ + RIS or Al.N to dttmniner diffcrUlC'fS umoog doses md \tf'lilf 'chic ('vs 'chkle, '...,' rolll'l dose within drug. 'vs medium dosti wilhio dlug). ANOVA usillg aU groups mtd to dctmnin l'<iffttttoC'-l':I II do8Nq1li\'aleots (11 v1dose C'C1ivalall of AU. .

Table 3
Click here to do'''''''loaj high resolution image

Tabl• 3. licrodamnge A$'l<ssment of third lumbar•r1ebrae

	V•.hld.	C.11-l:sf			AJnidrom•					
		IUD			0..1.U	n.:o	100			Al.If
C•H,	I S•t.S	J S•O)•	4 0 •07•	6.S.t-t' ..	)-t 0.8	S.Ooi08'	IJ O •1 1•		<O 0001	•O01
	Sl 8 t 4 S	, •Jt	dl) t .Sd	63f a 4 S	ff 6 J 4)	S.S•l4	S7S•2 a			
	O IJ •f 04	0))J f 04 •	1n-..11 O.•	Odl>•Oot..	f U •D ll7	D4$tDGa•	OSS•OIO•		<:IJ llMll	C:o

,_JkrodDllll@t p.amelcn u5C'SUd oo L3 va1cb111e following buUt cr-.N. cnck twnlbcr. Cr.Lt mt'9ll mek kfl3'h: ()Do:crack dcnroy (CrNllr1bcicullr boot •ca).. Dall iremt''.n t- SE. Sq>Ullle •''''.Y A.. OVA ruo using vm1+RJS or ALN 10 dtttn:nloe n tnet$ •t101 13 dol!ei mid VftllliJ vdtklt (•\'t vdtkle.1> vt low dose 'thin <k'll8o c vs mtdium dose vithin dn1@:1. ANOVA usins 111 groops us«l IO ddmnklt- di1fttmcts nt dou-tqttlvalmt•(no dost· cqtiv1Jt'tlt difftrtuct for thtst \'Iii Witt).

Table 4

Click here to do"""""loaj high resolution image

Table 4. Mechanical pr-op•rties of fourth lumbar vert•bra

	\'!':hkli!	Ri"l!ttr-•tn•ac			Alimilr...-(-c:.kcf				YEH •	
		DUS	0.10	,•,	D.ID	0.r0	IJl1			
	)TUJ.lff	'44JO:rfl	IO I	4 .1204	"G1.t 1l1	40f J 1161	41'-I 11•7			
GIlf&w:A	71W)I:Slf	'411 .t2'-1	ll07 :.TII•	ff ll:l?O•	MIS!.-'S4•	JJOS 4SI•	JUS:.504•			0"
	1.1i ,,,	114111141	I$ t. 10	lfot 117	171'.t 141	1644 :s.90	1tlStIN			
	141,t.OOl	1•11.00&	l tlt-110	16.t.OOI	1•71.00f	I l,t-ON	ISO a.OOS			
(6VffV) nwrrvi	410 t10	"4tJ.	SI).:t 4 7	«I i I 0	•ll 1.1•	.«9-s lS	•1Sa.11	Oll		
(BVnv)	0.047.t		OCMJ i.	O I.;.		OOJI s	001 'i			0"

SlflKll.8111 and n-.C«lal propttttln orl.4 \ltrttbnc body llUSltd tL lgCOlllptetd!>slt I.I. tJ4 ullltOltt- k)ad; BVIV, b'ltbKtlbr bone\-Ol1imcobc11i.1cd&omL2tais1oinorpZIOnry. ()ell we mc•1t: S& Sq>nnrcI IA'*)'ANOVAn111 us:illgVEB + IUS Of ALN dctmninc dl.ffcrcn«S among dosal: and \"tml!!\'dlit ('vsvchiiclc=). ANOVA us..U gro.1ptl.ISed coddmrlincdiOtrtnces 11cloff-c<1ttiv1lnll.t (tM>dote-cc(\U!llt:1ddiftttciicc(or UM'Jicvwillblcs).

Figure 1
Click here to do"""""loaj high resolution image

Figure 1

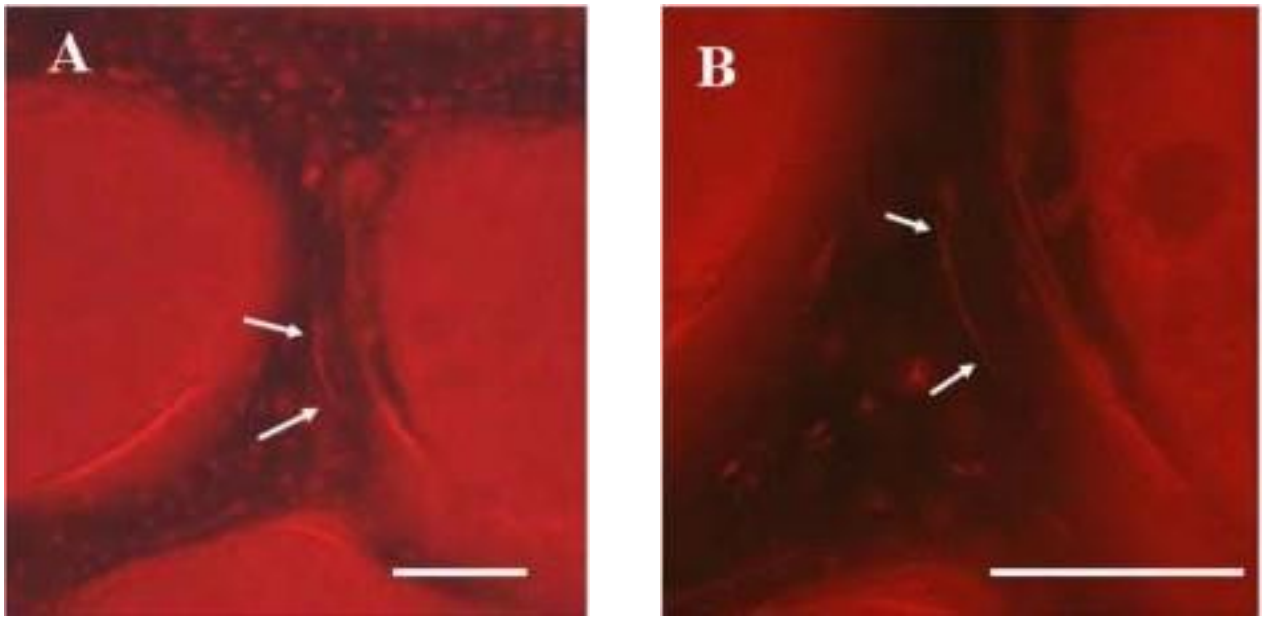

Figure 2
Click here to dow-1load high resolution image

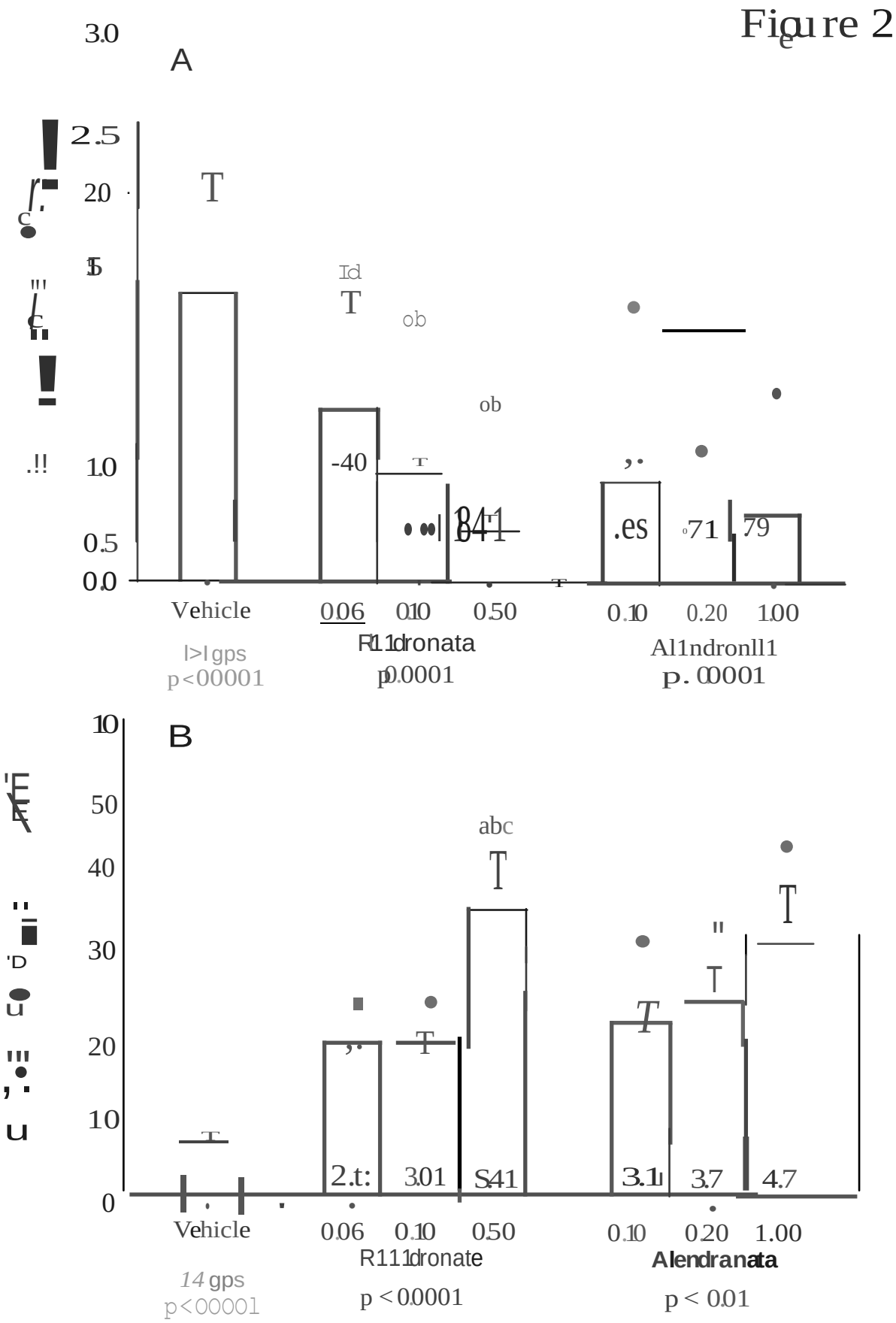

Figure3
Click here to do""""loaj high resolution image

Figure 3